JOURNAL OF APPLIED ELECTROCHEMISTRY 21 (1991) 973–981

Oxygen reduction on poly(4-vinylpyridine)-modified ordinary pyrolytic graphite electrodes with adsorbed cobalt tetra-sulphonated phthalocyanine in acid solutions

Z. Y. ZENG*, S. L. GUPTA, H. HUANG, E. B. YEAGER

Case Center for Electrochemical Sciences and the Department of Chemistry, Case Western Reserve University, Cleveland, Ohio 44106, U.S.A.

Received 24 July 1990

Poly(4-vinylpyridine) (PVP) has been used to modify ordinary pyrolytic graphite (OPG) electrodes with adsorbed cobalt tetra-sulphonated phthalocyanine (CoTsPc) in acid solutions. These modified electrodes were prepared in different manners and characterized by cyclic voltammetry. Their electrocatalytic activity for oxygen reduction and stability in 0.05 M H_2SO_4 solutions was examined at room temperature. The OPG/CoTsPc/PVP modified electrodes were found to be more active for oxygen reduction in 0.05 M H_2SO_4 solutions as compared to the electrode with adsorbed CoTsPc on OPG without PVP. The increase in activity is due to the formation of an adduct between PVP and CoTsPc. U.v.–visible and FTIR studies provide evidence for such adduct formation. Over a 10 h period the activity of the OPG/CoTsPc/PVP system was essentially constant while that of OPG/CoTsPc without polymer decreased by a substantial amount (about 37%). The PVP layer inhibits the diffusion of the CoTsPc and/or Co out of the complex into the solution phase. The stability of the OPG/CoTsPc/PVP system may also be due to low solubility of the adduct between PVP and CoTsPc in a 0.05 M H_2SO_4 solution. Thicker films of PVP decreased the diffusion limiting oxygen reduction current. The effect of pH of the electrolyte solution on the activity of such PVP-modified electrodes for oxygen reduction has also been investigated.

1. Introduction

Polymer coatings have been used by many researchers to incorporate various metal complexes in order to improve the activity and stability on electrode surfaces. Poly(4-vinylpyridine) (PVP) is one of many investigated polymers. Oyama, Anson and co-workers have reported that transition metal complexes can be incorporated in protonated PVP films and can be used to catalyse or mediate electron transfer between the electrode surface and reactants present in the solution [1–6]. Bartak *et al.* studied the electrodeposition of platinum microparticles in PVP films on glassy carbon electrodes and reported that this type of electrode exhibited good activity with regard to the generation of hydrogen [7]. Orlov *et al.* studied the electrochemical behaviour and electrocatalytic properties of the complex of Cu^{2+} with PVP [8].

The present investigation deals with PVP-modified ordinary pyrolytic graphite (OPG) electrodes with adsorbed cobalt tetrasulphonated phthalocyanine (CoTsPc) for oxygen reduction in 0.05 M H_2SO_4 solutions. Such electrodes have been characterized by linear sweep voltammetry. The influence of thickness of the PVP film, pH of the electrolyte and the method of preparation of the modified electrodes have been investigated for oxygen reduction activity. Adducts formed between PVP and CoTsPc have been isolated from acid and neutral solutions and examined for their activity for oxygen reduction. FTIR and u.v.–visible spectroscopic techniques have been used to identify the adducts.

2. Experimental details

2.1. *Chemicals*

CoTsPc was synthesized and purified according to the method of Weber and Busch [9]. It was further purified by dialysis in distilled water to remove various uncomplexed ions. The solid was obtained after evaporation of the water under reduced pressure. PVP (molecular weight = ~50 000) was obtained from Polyscience Inc. The H_2SO_4 (ultrapure reagent, Baker), CH_3OH (spectrophotometric grade, Aldrich), cobalt phthalocyanine (CoPc) (Kodak), KH_2PO_4, Na_2HPO_4 (analysed reagent, Baker) and dimethyl sulphoxide (DMSO) (Fisher) were used as received. All the aqueous solutions were prepared in ultrapure water from reverse osmosis distillation [10]. PVP solutions (8×10^{-5} to 8×10^{-3} g cm^{-3}) were prepared by dissolving the PVP powder in CH_3OH.

* On leave from the Department of Chemical Engineering, Guangdong Institute of Technology, Guangzhou, People's Republic of China.

0021-891X/91 $03.00 + .12

2.2. *Electrochemical cell and instrumentation*

A three-compartment cell was used. A gold foil (99.9% pure) and a saturated calomel electrode (SCE) served as counter and reference electrodes respectively. An OPG disc (area = 0.196 cm^2, from Union Carbide Co., Parma, Ohio), compression molded in Kel-F and screwed into a Teflon holder, was used as a working electrode. Before every experiment the electrode surface was polished with a 0.05 μm Al_2O_3 emulsion (Buehler) and placed in an ultrasonic cleaning bath for 5 min and finally rinsed with pure water. Electrochemical equipment included a RDE-3 potentiostat, an ASR-2 rotator (both from Pine Instruments, Inc.) and an X–Y recorder (Houston Instruments). Infrared spectra were obtained with a Michelson-Genzel type FTIR instrument (IR/98, IBM Instruments, Inc.) using diffuse-reflectance infrared Fourier transform (DRIFT) spectroscopy in KBr matrix and a diffuse-reflectance accessory from Spectro-Tech, Inc. The i.r. data are presented in Kubelka-Munk units [11]. A u.v.-vis. spectrophotometer (Cary 2300, Varian Instruments) was used for u.v.-visible measurements.

2.3. *Isolation of adducts from the solution*

Adduct I was obtained by mixing 13 cm^3 of 1.2 mg cm^{-3} PVP solution in pure methanol with 2 cm^3 of 10 mg cm^{-3} CoTsPc solution in *pure water*. After the mixture was kept at 60° C for 5 h, the solvent was removed. The solid thus obtained was vacuum dried at 60° C overnight. It was washed with pure water and methanol, respectively, and finally dried under vacuum at 60° C overnight.

Adduct II was obtained by mixing 3 cm^3 of 3.3 mg cm^{-3} PVP solution in pure methanol and 15 cm^3 of 1 mg cm^{-3} CoTsPc solution in 0.05 M H_2SO_4. The dark blue precipitate appeared immediately after mixing, and was filtered and washed with pure water and methanol, respectively, and dried in vacuum at 50° C overnight.

2.4. *Preparation of modified electrodes*

The modified electrodes were prepared in three different ways:

2.4.1. OPG/CoTsPc/PVP. The OPG electrode was immersed in 1 × 10^{-4} M CoTsPc in air-saturated water for 15 min without potential control with the electrode rotating at ~30 r.p.m. The electrode was removed and washed with pure water. It was then immersed in a PVP solution (8 × 10^{-4} g cm^{-3} in methanol) for 20 min, then removed from the PVP solution and the solvent was allowed to evaporate at room temperature. Finally, the electrode was rinsed with pure water. For this electrode, the CoTsPc was expected to be between the OPG and PVP layer.

2.4.2. OPG/(CoTsPc + PVP). The OPG electrode was immersed in a solution containing 1 × 10^{-4} M CoTsPc and 8 × 10^{-4} g cm^{-3} PVP in 1:9 water/methanol mixture saturated with air for 20 min with the electrode rotating at ~30 r.p.m. The electrode was then removed from the solution and washed with pure water. This electrode was expected to have the CoTsPc in the PVP layer.

2.4.3. OPG/PVP/CoTsPc. The OPG electrode was first coated with a thin film of PVP formed by evaporating the solvent from ~6 μ dm^{-3} of PVP solution (8 × 10^{-4} g cm^{-3} in methanol) at room temperature. After rinsing with pure water the electrode was then immersed in 1 × 10^{-4} M CoTsPc solution in water (air-saturated) for 15 min with the electrode rotating at ~30 r.p.m. The electrode was finally washed with water. In this instance the CoTsPc was expected to be on top of the PVP layer.

3. Results and discussion

3.1. *Cyclic voltammetry*

Cyclic voltammograms with OPG electrodes were obtained in nitrogen or oxygen saturated 0.05 M H_2SO_4 solutions. Figure 1 shows the cyclic voltammograms on OPG and OPG/PVP electrodes in nitrogen-saturated solutions. It indicates that the thin film of PVP on the OPG electrode surface do not cause any significant change in electrochemical behavior of the OPG electrode in acid solutions. Peak c′ and c corresponds to the redox behavior of the quinone/hydroquinone functional group on the OPG surface [12]. Figure 2 shows the cyclic voltammograms on OPG/CoTsPc and OPG/PVP/CoTsPc electrodes in nitrogen-saturated 0.05 M H_2SO_4 solutions. According to the [13] the peaks a′, b′ and d′ can be assigned as follows:

Peak a′: Co(I)TsPc(−2)/Co(I)TsPc(−3), H^+
Peak b′: Co(II)TsPc(−2)/Co(I)TsPc(−2), H^+
Peak d′: Co(III)TsPc(−2)/Co(II)TsPc(−2)

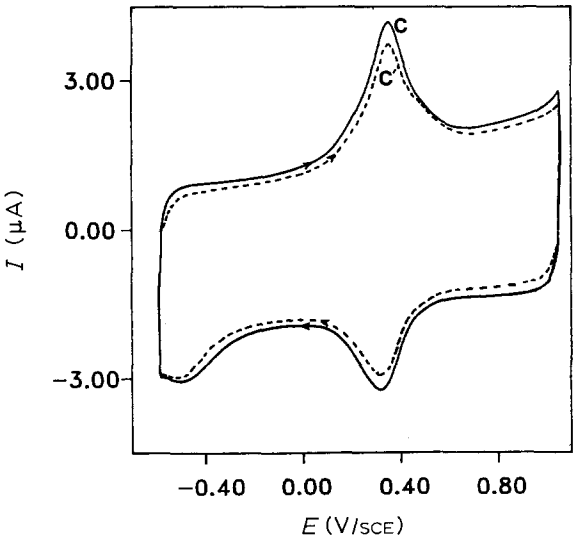

Fig. 1. Cyclic voltammograms on OPG (– – –) and OPG/PVP (——) electrodes in N_2-saturated 0.05 M H_2SO_4 solutions. Scan rate: 200 mV s^{-1}.

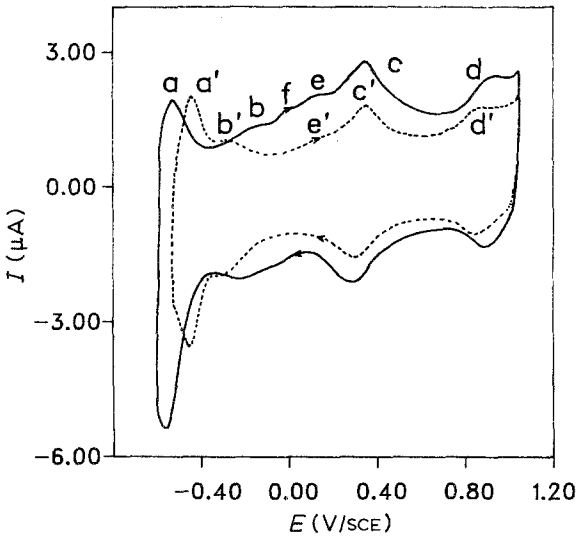

Fig. 2. Cyclic voltammograms on OPG/CoTsPc (– – –) and OPG/PVP/CoTsPc (——) electrodes in N_2-saturated 0.05 M H_2SO_4 solutions. Scan rate: 200 mV s^{-1}.

The peak c′ and c in Fig. 2 corresponds to peak c′ and c in Fig. 1. The peak e and e′, with and without PVP, as well as some additional small peaks with PVP in Fig. 2, are not clear at present. The potentials of peaks a, b and d with PVP are somewhat different from the peak potentials of a′, b′ and d′ without PVP, indicating some interaction of PVP with CoTsPc. Similar changes are observed with OPG/CoTsPc/PVP and OPG/(CoTsPc + PVP) modified electrodes.

Figures 3 and 4 show the cyclic voltammograms with OPG, OPG/PVP, OPG/CoTsPc and OPG/CoTsPc/PVP electrodes in oxygen-saturated 0.05 M H_2SO_4 solutions. Figure 3 shows that the PVP film on the surface of the OPG electrode does not cause a significant change in either the peak potential or the peak current for oxygen reduction, but does show some minor changes which suggest that the transport of oxygen is somewhat inhibited. Figure 4 shows that the peak potential of oxygen reduction on the OPG/CoTsPc electrode is more positive than that on OPG alone, and further positive shift in the peak potential

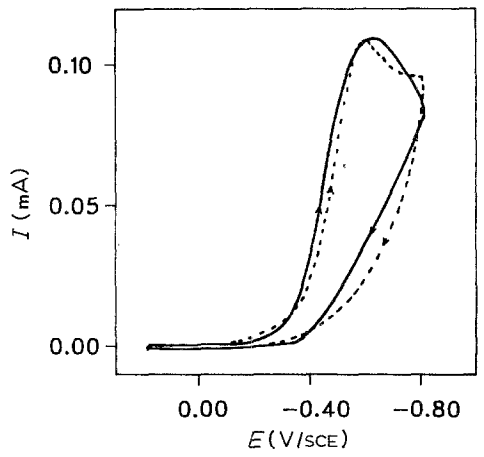

Fig. 3. Cyclic voltammograms on OPG (– – –) and OPG/PVP (——) electrodes in O_2-saturated 0.05 M H_2SO_4 solutions. Scan rate: 100 mV s^{-1}.

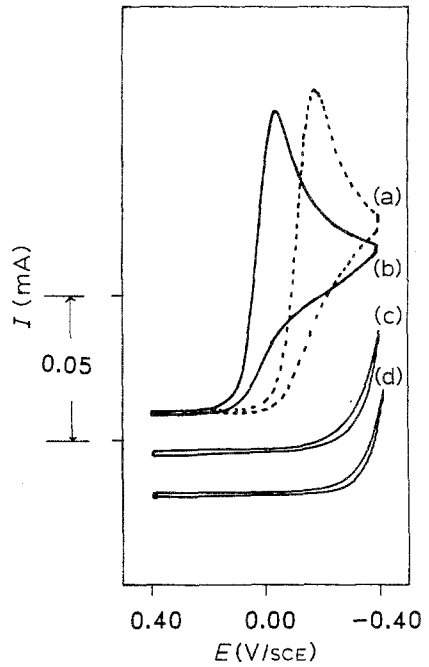

Fig. 4. Cyclic voltammograms on various electrodes in O_2-saturated 0.05 M H_2SO_4 solutions. (a) OPG/CoTsPc, (b) OPG/CoTsPc/PVP, (c) OPG/PVP and (d) OPG. Scan rate: 100 mV s^{-1}.

is obtained when the OPG/CoTsPc electrode is coated with a thin layer of PVP (about 0.14 V). It is thus clear that the OPG/CoTsPc/PVP electrode exhibits higher catalytic activity for oxygen reduction than OPG/CoTsPc in 0.05 M H_2SO_4 solutions.

3.2. *Oxygen reduction*

Figure 5 shows the current-potential curves for oxygen reduction at OPG/CoTsPc and OPG/CoTsPc/PVP electrodes at different rotation speeds in oxygen-saturated 0.05 M H_2SO_4 solutions. The half-wave potential ($E_{1/2}$) shifts by about 0.11 V more positive for the PVP-modified electrode than the unmodified electrode, but the limiting current is nearly the same, indicating no inhibition in the diffusion of oxygen through the PVP film of such thickness.

For a rotating disc electrode experiment involving a totally irreversible electrode process which is first order for the reactant, the measured current i is given by [14]

$$\frac{1}{i} = \frac{1}{i_k} + \frac{1}{i_d} = \frac{1}{i_k} + \frac{1}{B\omega^{1/2}} \qquad (1)$$

where i_k is the kinetic current, i.e. the current in the absence of mass transport control, i_d is the diffusion limiting current, ω is the rotation rate and B is a constant independent of rotation rate. An expression for i_d is given by

$$i_d = B\omega^{1/2} \qquad (2)$$

$$B = 0.62nFAC_0^* D_0^{2/3} \nu^{-1/6} \qquad (3)$$

where n is the overall number of electrons transferred per oxygen molecule, A is the electrode area, C_0^* is the bulk concentration of the reactant, D_0 is the diffusion

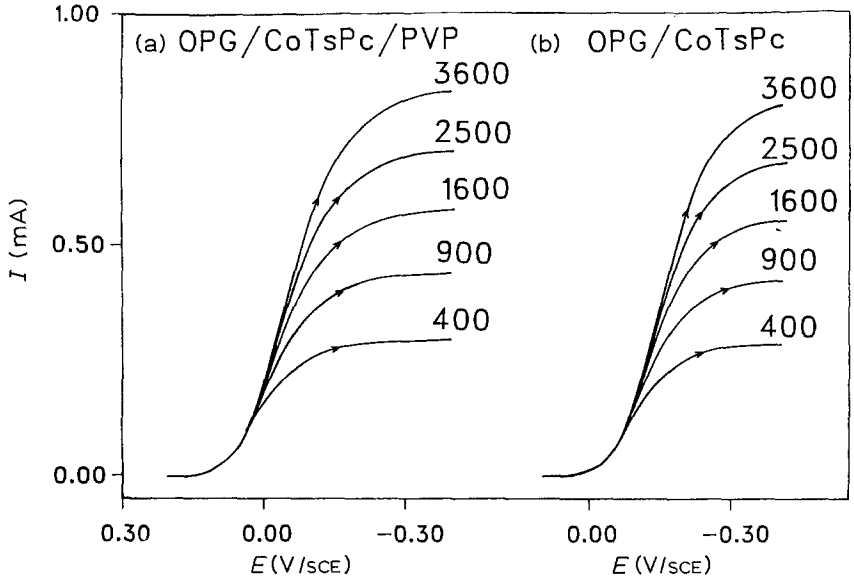

Fig. 5. Current–potential curves for oxygen reduction on rotating (a) OPG/CoTsPc/PVP and (b) OPG/CoTsPc disc electrodes in O_2-saturated 0.05 M H_2SO_4 solutions. Scan rate: 10 mV s^{-1}. The number above each curve indicates the corresponding rotation rate in r.p.m.

coefficient of the reactant and v is the kinematic viscosity.

According to Equation 1, a plot of i^{-1} against $\omega^{-1/2}$ should be linear with an intercept equal to i_k^{-1} and slope equal to $1/B$. Thus i_k and B can be obtained.

Figure 6 shows the plots of i^{-1} against $\omega^{-1/2}$ from the data in Figure 5b for oxygen reduction on the OPG/CoTsPc electrode. The i_k calculated from intercepts are shown in Table 1.

For a polymer-modified electrode, as for example the OPG/CoTsPc/PVP electrode, the limiting current (i_{lim}) for oxygen reduction is given by [14, 15]

$$\frac{1}{i_{lim}} = \frac{1}{i_f} + \frac{1}{i_d} = \frac{1}{i_f} + \frac{1}{B\omega^{1/2}} \quad (4)$$

where i_f is the current controlled by oxygen diffusion through the polymer film. A plot of $(i_{lim})^{-1}$ against $\omega^{-1/2}$ should be linear and i_f^{-1} can be obtained from the intercept.

The measured current, i, at any point on the current-voltage curve is given by

$$\frac{1}{i} = \frac{1}{i_k} + \frac{1}{i_f} + \frac{1}{B\omega^{1/2}} \quad (5)$$

According to Equation 5, a plot of i^{-1} against $\omega^{-1/2}$ should be linear and $(1/i_k + 1/i_f)$ can be obtained from the intercept. As the i_f^{-1} can be obtained from the plot of $(i_{lim})^{-1}$ against $\omega^{-1/2}$, so i_k can be calculated for the modified electrode.

Figures 7 and 8 show the plots of $(i_{lim})^{-1}$ against $\omega^{-1/2}$ and i^{-1} against $\omega^{-1/2}$, respectively. From the data in Fig. 5a for oxygen reduction on the OPG/CoTsPc/PVP electrode, the i_k values can be obtained and are listed in Table 1.

The data from Table 1 shows that the kinetic current is much higher on the OPG/CoTsPc/PVP electrode than on the OPG/CoTsPc electrode at the same potential. The enhancement factors [17] (see Table 1) are quite large.

From the Figs 6 and 8, we find that the plots of i^{-1} against $\omega^{-1/2}$ at various potentials are linear and parallel. This confirms that the rate of oxygen reduction on the OPG/CoTsPc/PVP electrode is first order with respect to oxygen, as is the case for the OPG/CoTsPc electrode. The B values determined from Figs 6 and 8 are 1.46×10^{-2} mA (r.p.m.)$^{-1/2}$ and 1.47×10^{-2} mA (r.p.m.)$^{-1/2}$, respectively. These values

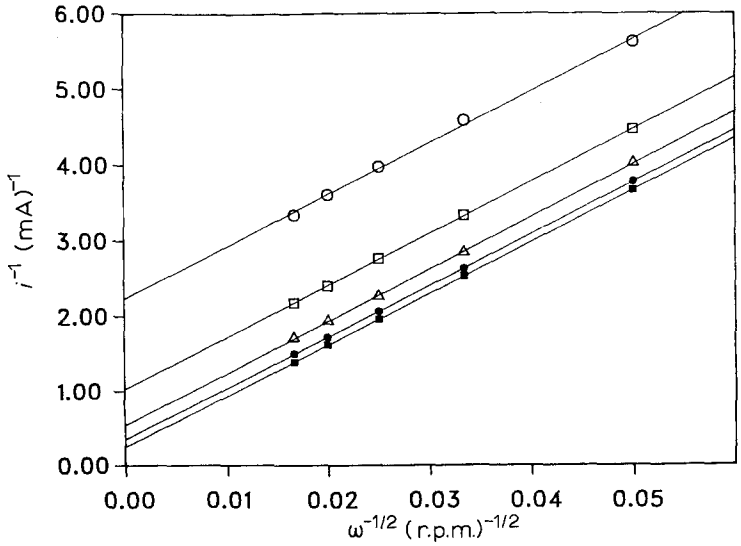

Fig. 6. Koutecky-Levichs plots for oxygen reduction on OPG/CoTsPc electrode at potentials: (○) −0.14, (□) −0.18, (△) −0.22, (●) −0.26 and (■) −0.30 V. Data from Fig. 5(b).

Table 1. Kinetic currents at different potentials for oxygen reduction on various electrodes in 0.05 M H_2SO_4 solutions

E (V/SCE)	i_k (mA cm^{-2})				
	OPG/PVP/CoTsPc	OPG/(PVP + CoTsPc)	OPG/CoTsPc/PVP	OPG/CoTsPc	E_F^*
−0.14	10.63	12.07	17.04	2.28	7.47
−0.18	19.85	20.76	33.11	4.95	6.69
−0.22	34.15	38.16	58.92	9.43	6.25
−0.26	72.58	72.78	82.83	14.49	5.71

* E_F (enhancement factor) = [i_k on (OPG/CoTsPc/PVP)/i_k on (OPG/CoTsPc)].

agree very well with the calculated value (1.42×10^{-2} mA (r.p.m.)$^{-1/2}$) [12] from Equation 3 for $n = 2$, indicating that oxygen reduction proceeds through a 2-electron pathway leading to H_2O_2 on these electrodes.

Figure 9 shows the disc potential E against log (i_k) plot (Tafel plot) for the modified electrode. It exhibits linear behaviour over two decades with a slope of −130 mV decade^{-1}. The upper section of the plot at potentials numerically greater than −0.20 V is limited by the accuracy with which the intercepts in Fig. 8 could be determined. This value is close to the theoretically expected value of −118 mV decade^{-1} for an apparent transfer coefficient $\alpha = 0.5$ with a first one electron transfer rate controlling step at 25° C, i.e.

$$O_2 \text{ (ads)} + e^- \longrightarrow O_2^- \text{ (ads)}.$$

This supports the mechanism for oxygen reduction on graphite proposed by Morcos and Yeager [18].

3.3. *The effect of the polymer film on the O_2 reduction kinetics*

Figure 10 shows the comparison of polarization curves for oxygen reduction at a rotation speed of

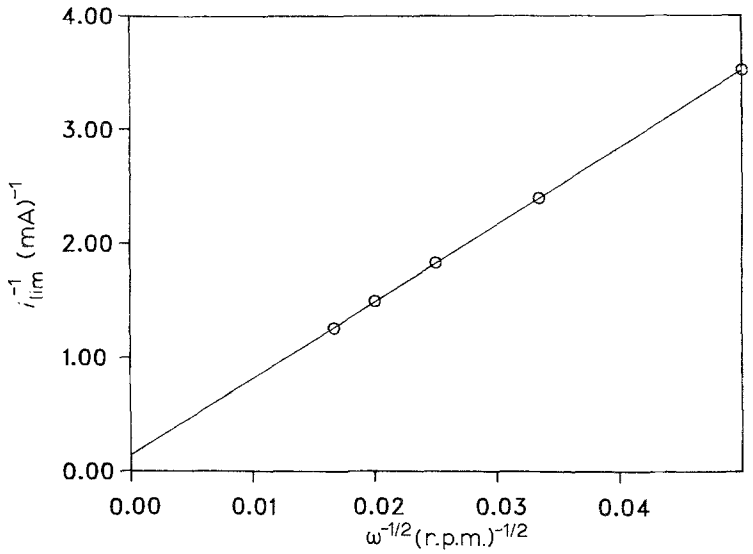

Fig. 7. Plot of $(i_{lim})^{-1}$ against $\omega^{-1/2}$ for oxygen reduction on OPG/CoTsPc/PVP electrode in O_2-saturated 0.05 M H_2SO_4 solutions. Scan rate: 10 mV s^{-1}.

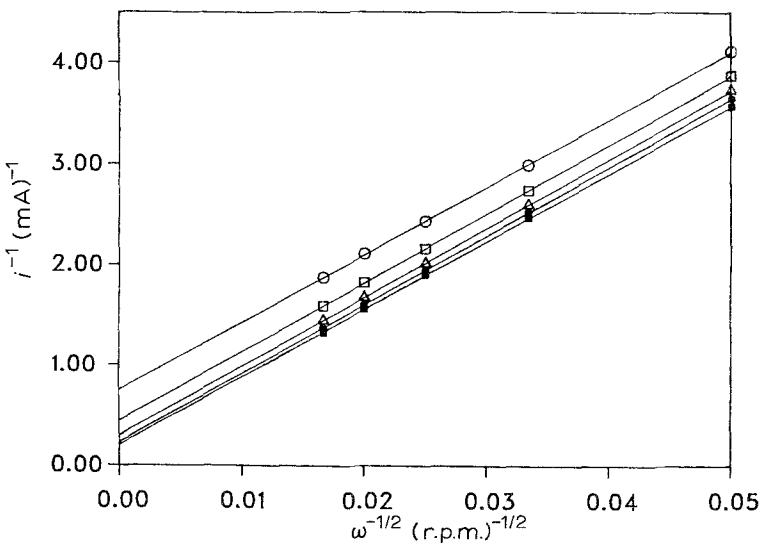

Fig. 8. Koutecky-Levichs plots for oxygen reduction on OPG/CoTsPc/PVP electrode at potentials: (○) −0.10, (□) −0.14, (△) −0.18, (●) −0.22 and (■) −0.26 V. Data from Fig. 5(a).

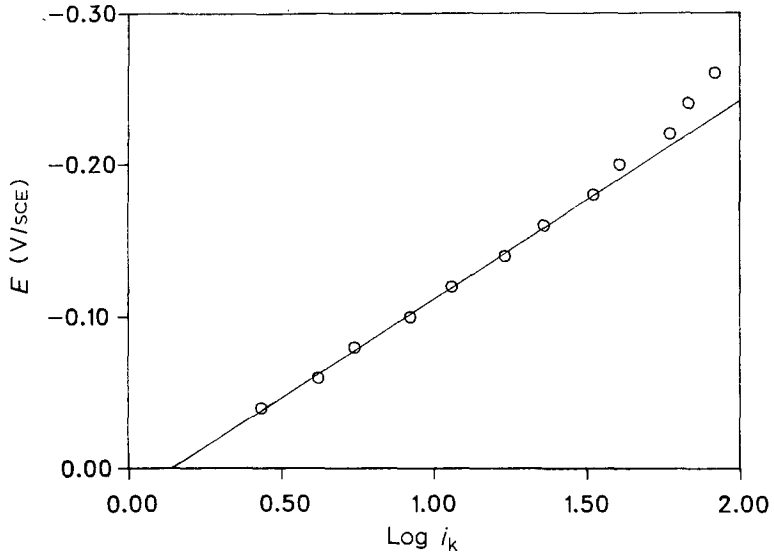

Fig. 9. Tafel plot for oxygen reduction on OPG/CoTsPc/PVP electrode in O_2-saturated 0.05 M H_2SO_4 solutions. Data from the intercepts in Fig. 8.

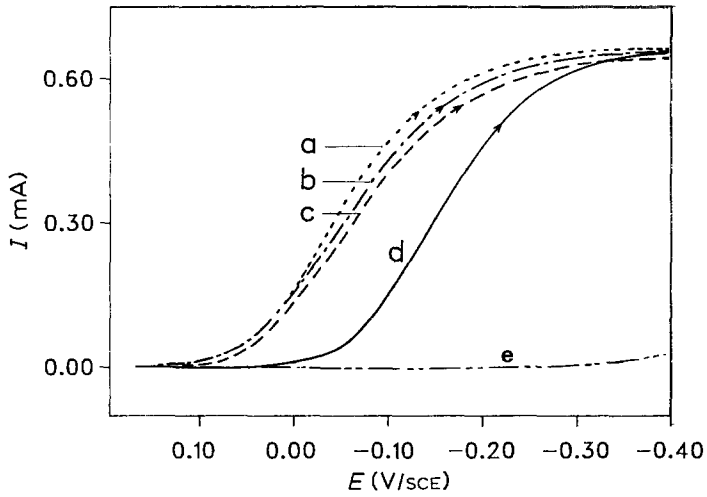

Fig. 10. Rotating-disc voltammograms for oxygen reduction in O_2-saturated 0.05 M H_2SO_4 solutions. (a) OPG/CoTsPc/PVP (···), (b) OPG/(PVP + CoTsPc) (-·-·-·-), (c) OPG/PVP/CoTsPc (- - -), (d) OPG/CoTsPc (——) and (e) OPG (—··—··). Rotation rate: 2500 r.p.m., scan rate: 10 mV s^{-1}.

2500 r.p.m. for various PVP-modified electrodes in 0.05 M H_2SO_4 solutions saturated with oxygen. The curves a, b, and c with polymer films are close to each other and the rising portions of the oxygen reduction waves shift positive relative to the curve d without the film. The kinetic currents i_k for oxygen reduction on OPG/CoTsPc/PVP, OPG/(CoTsPc + PVP) and OPG/PVP/CoTsPc electrodes are also listed in Table 1; these are close to each other. In order to explain these results and the fact that the OPG/CoTsPc electrode modified by PVP exhibits higher electrocatalytic activity for oxygen reduction in acid medium, the interaction between CoTsPc and PVP must be considered.

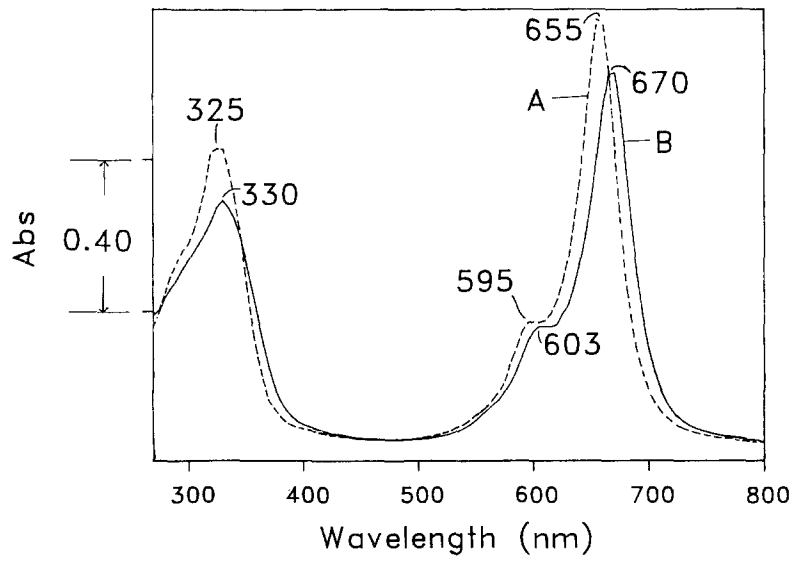

Fig. 11. U.v.-visible absorption spectra for (a) 1 × 10^{-4} M CoTsPc and (b) 1 × 10^{-4} M CoTsPc + 8 × 10^{-4} g cm^{-3} PVP in 1:9 water/methanol mixture. Cell length: 1.00 cm. The number near a peak indicates the corresponding peak position in nanometre.

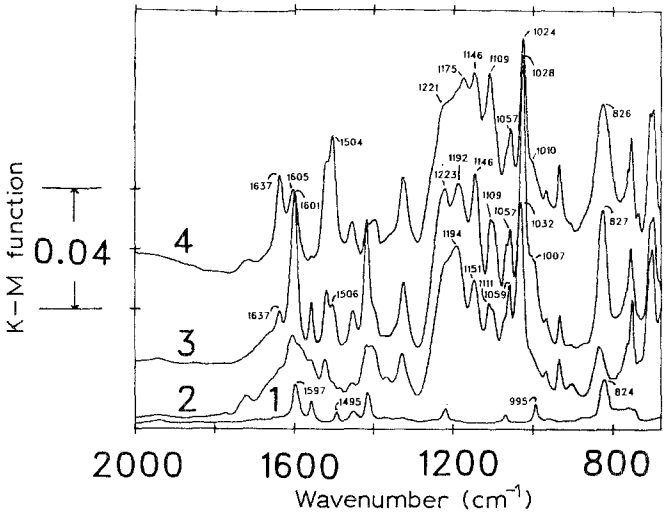

Fig. 12. Diffuse reflectance FTIR spectra of (1) PVP, 0.1 wt %; (2) CoTsPc, 0.5 wt %; (3) adduct I, 0.6 wt % and (4) adduct II, 0.6 wt % in KBr. Grinding time: 5 min. The K-M function = $(1 - R)^2/2R$, where R is the reflectance (see [11]). The small number in the figure indicates the corresponding peak position in cm^{-1}.

3.4. *Interaction between PVP and CoTsPc*

In studies of oxygen reduction electrocatalysis involving transition metal macrocycles, the nature of the chelete and particularly the centre ion play a decisive role [19]. In the polymer-modified electrode, however, the interactions between the transition metal macrocycle and the polymer must be considered. These interactions may include the chemical bonding and electrostatic interactions. With CoTsPc-PVP-modified electrodes, it is possible that both chemical and electrostatic interactions play an important role. Figure 11 shows the u.v.-visible absorption spectra obtained with solutions of 1×10^{-4} M CoTsPc and 1×10^{-4} M CoTsPc + 8×10^{-4} g cm^{-3} PVP both in 1:9 water/methanol mixtures. The 325 nm, 595 nm and 655 nm absorption bands for the CoTsPc solution without PVP shift to 330, 603 and 670 nm, respectively, for the same solution with PVP.

Figure 12 gives the infrared spectra of PVP, CoTsPc and the adducts formed between CoTsPc and PVP in a KBr matrix using diffuse-reflectance infrared Fourier transform spectroscopy. It is seen from Table 2 that the absorption of PVP at 1597 cm^{-1} for $\nu_{C=C,C=N}$ of the PVP pyridine ring shifts to 1637 cm^{-1} in both adduct I and adduct II. This supports the coordination between pyridine of the PVP and cobalt of CoTsPc. The band around 1601 cm^{-1} in adduct I and around 1605 cm^{-1} in adduct II may correspond to the uncoordinated pyridine of the PVP in the adducts. The absorption peaks due to the $\nu_{C=C}$, δ_{CH} (in plane) and δ_{CH} (out of plane) of PVP also shift to a higher wavenumber by 9–11, 12–15 and 2–3 cm^{-1}, respectively, in the adducts. The results summarized in Table 2 are very similar to the results obtained by Kurimura *et al.* [20] for the complexes of PVP with cis-$[Co(en)_2Cl_2]Cl$ and cis-$[Co(trien)Cl]Cl_2$ and suggest the coordination of cobalt in CoTsPc with the pyridine nitrogen of PVP through the axial position of the transition metal.

Although the peak shifts for both adduct I and adduct II are similar, as seen from Table 2, there are certain differences in the infrared spectra for the two adducts. The absorption peaks around 1194 cm^{-1} and 1032 cm^{-1} for asymmetric and symmetric stretching vibrations of $-SO_3^-$ in CoTsPc shift to lower wavenumbers, 1175 and 1024 cm^{-1}, respectively, in adduct II. It is obvious that the shift of these peaks results from some kind of interaction of the PVP polymer with the $-SO_3^-$ group in CoTsPc. This may be explained on the basis that besides the coordination of pyridinonitrogen of PVP with cobalt in CoTsPc, there is also an electrostatic interaction between the $-SO_3^-$ group and protonated pyridine units which are uncoordinated in the PVP. If 0.05 M H_2SO_4 is added to the solution containing 8×10^{-4} g cm^{-3} PVP and

Table 2. Assignment of some spectral features of DRIFT spectra of PVP, adduct I and adduct II (in KBr)

Ligand and adducts	*Assignment* (cm^{-1})			
	$\nu_{C=C,C=N}$	$\nu_{C=C}$	δ_{CH} *(in plane)*	δ_{CH} *(out of plane)*
PVP	1597	1495	995	824
Adduct I	1637, 1601	1506	1007	827
Adduct II	1637, 1605	1504	1010	826

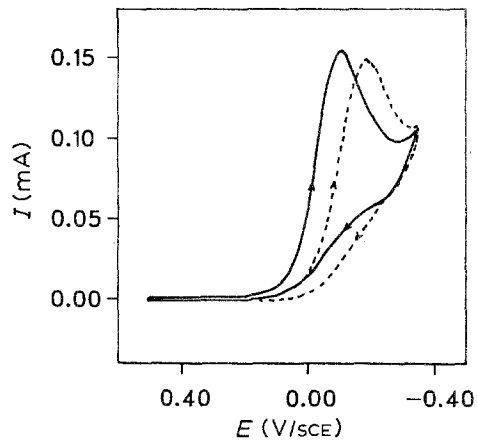

Fig. 13. Cyclic voltammograms on OPG/CoPc/PVP (——) and OPG/CoPc (– – –) electrodes in O_2-saturated 0.05 M H_2SO_4 solutions. Scan rate: 10 mV s^{-1}.

Table 3. Voltammetric peak potentials (SCE) for oxygen reduction in various electrolyte solutions

Electrolyte	E_{pc} (V) *OPG/CoTsPc*	E_{pc} (V) *OPG/CoTsPc/PVP*	E_{pc} (V) *OPG/PVP/CoTsPc*
0.05 M H_2SO_4	−0.19	−0.05	−0.07
Phosphate buffer (pH 7.4)	−0.40	−0.45	−0.57
0.1 M NaOH	−0.40	−0.44	−0.52

1×10^{-4} M CoTsPc in 1:9 water/methanol mixture, a dark blue precipitate appears immediately corresponding to the formation of adduct II.

When either of the adducts is adsorbed on the OPG electrode from its solution in DMSO, it shows much better catalytic activity for oxygen reduction in 0.05 M H_2SO_4 solutions than the OPG electrode with only adsorbed CoTsPc and closely similar activity to the PVP-modified OPG electrode with adsorbed CoTsPc.

Cobalt phthalocyanine, which has no $-SO_3^-$ group, was used to replace CoTsPc for comparison. The preparation of the modified electrode for CoPc is the same as for CoTsPc except the CoPc was adsorbed from a DMSO solution. Figure 13 shows the cyclic voltammograms with OPG/CoPc/PVP and OPG/CoPc electrodes in oxygen-saturated 0.05 M H_2SO_4 solutions. The catalytic activity for oxygen reduction is higher on the OPG/CoPc/PVP electrode than on the OPG/CoPc electrode. This can also be explained by the formation of an adduct between CoPc and PVP on the OPG electrode surface. The only strong interaction between the CoPc and PVP in this adduct is the coordination of the pyridine in PVP with the Co in CoPc.

3.5. *Influence of pH on catalytic activity for oxygen reduction*

Table 3 shows the peak potentials (E_{pc}) for oxygen reduction, which are obtained from cyclic voltammograms on OPG/CoTsPc, OPG/CoTsPc/PVP and OPG/PVP/CoTsPc electrodes in 0.05 M H_2SO_4, phosphate buffer and 0.1 M NaOH solutions saturated with oxygen. For a totally irreversible system the peak potentials are expected to be a linear function of ln (k^0), where k^0 is the first order standard rate constant [21]. The CoTsPc-PVP-modified OPG electrode exhibits higher catalytic activity for oxygen reduction, as compared with the OPG/CoTsPc electrode in acid solutions. In the neutral or alkaline solution, however, a similar CoTsPc-PVP modified electrode inhibits oyxgen reduction as compared to the CoTsPc modified electrode without PVP. This may be due to the formation of an unprotonated, poorly conducting, film of PVP on the electrode surface which considerably reduces the diffusion of oxygen through the film and increases the ohmic resistance. Similar inhibition was obtained with an OPG electrode coated with a PVP layer without the macrocycle.

3.6. *Influence of the thickness of PVP films*

In order to investigate the effect of the thickness of the PVP film on the electrode surface on catalytic activity for oxygen reduction, the thickness of the PVP film coated on the electrode surface was varied by changing the concentration of the PVP solution, keeping the solution volume constant. The results are given in Table 4. In the PVP film thickness range between 0.002 and 0.1 μm, the differences in $E_{1/2}$ are practically negligible. However, when the thickness of the PVP film increases further, the $E_{1/2}$ shifts negatively and the i_d decreases as shown in Table 4 for the OPG/PVP/CoTsPc electrode.

3.7. *Catalytic stability of the CoTsPc-PVP-modified electrode*

The OPG/CoTsPc/PVP and OPG/CoTsPc electrodes were used for the comparison of the catalytic stability for oxygen reduction in oxygen-saturated 0.05 M H_2SO_4 solutions. Oxygen was blown through the solution continuously and the electrode was rotated at 2500 r.p.m. maintaining the electrode potential at $E_{1/2}$. Over a 10 h period, the activity of the OPG/CoTsPc/PVP system was essentially constant while that of OPG/CoTsPc (no polymer) decreased substantially (~37%) indicating that the PVP layer prevents the diffusion of the CoTsPc and/or cobalt in the complex into the solution. The other interpretation of this effect may be due to the fact that the adduct formed between PVP and CoTsPc is insoluble in a 0.05 M H_2SO_4 solution.

Table 4. The effect of thickness (t)† of PVP film on OPG electrode with adsorbed CoTsPc on catalytic activity for oxygen reduction in 0.05 M H_2SO_4 solutions. (Rotation rate, 2500 r.p.m.; scan rate, 10 mV s^{-1})

t (μm)	*0*	*0.002*	*0.01*	*0.02*	*0.1*	*0.2*
C^* (mol cm^{-2})	0	1.7×10^{-9}	8.5×10^{-9}	1.7×10^{-8}	8.5×10^{-8}	1.7×10^{-7}
$E_{1/2}$ (V)	−0.175	−0.078	−0.076	−0.067	−0.075	−0.088
i_d (mA)	0.645	0.645	0.640	0.640	0.620	0.620

* C = concentration of PVP unit on the OPG surface.
† The thickness of PVP film was estimated approximately from the bulk density of PVP (0.85 g cm^{-3}).

4. Conclusion

The PVP-modified OPG electrode with adsorbed CoTsPc exhibits higher catalytic activity for oxygen reduction than the OPG electrode with only adsorbed CoTsPc in 0.05 M H_2SO_4 solutions. This may be due to the formation of an adduct between PVP and CoTsPc which is more active and more stable than the CoTsPc. However, a similar PVP-modified electrode exhibits inhibition for oxygen reduction in neutral and alkaline electrolytes.

PVP forms a protonated porous conducting film on the OPG electrode surface in acid solutions where the permeability of oxygen through the film is large. In neutral and alkaline solutions the PVP forms an unprotonated, poorly conducting, film on the OPG electrode surface which considerably reduces the diffusion of oxygen through the film and increases the ohmic resistance. Over a limited thickness range of the PVP film (0.002 to 0.1 μm), there is practically no significant change in the catalytic activity for oxygen reduction in acid media.

Acknowledgements

This work was supported by the U.S. Department of Energy through a subcontract with Lawrence Berkeley Laboratory as well as by the U.S. Office of Naval Research and Gas Research Institute.

References

[1] N. Oyama and F. C. Anson, *J. Am. Chem. Soc.* **101** (1979) 3450.
[2] *Idem., J. Electrochem. Soc.* **127** (1980) 247.
[3] *Idem., Anal. Chem.* **52** (1980) 1192.
[4] T. Shimomuta, N. Oyama and F. C. Anson, *J. Electroanal. Chem.* **112** (1980) 265.
[5] N. Oyama, T. Shimomuta, K. Shigehara and F. C. Anson, *ibid.* **112** (1980) 271.
[6] K. Shigehara, N. Oyama and F. C. Anson, *Inorg. Chem.* **20** (1981) 518.
[7] D. E. Bartak, B. Kazee, K. Shimazu and T. Kuwana, *Anal. Chem.* **58** (1986) 2756.
[8] S. B. Orlov, M. R. Tarasevich, V. A. Bogdanovskaya and V. S. Pshezhetskii, *Elektrokhimiya* **22** (1986) 768.
[9] T. H. Weber and D. H. Busch, *Inorg. Chem.* **4** (1965) 469.
[10] The apparatus and technique is a modified version by Dr B. Cahan of a system previously reported by R. Gilmont and S. J. Silvis in *Am. Lab.* **6** (1974) 46.
[11] M. P. Fuller and P. R. Griffths, *Anal. Chem.* **50** (1978) 1906.
[12] D. Chu, Ph.D. Thesis, Case Western Reserve University (1989) p. 28.
[13] S. Zecevic, B. Simic-Glavaski, E. Yeager A. B. P. Lever and P. C. Minor, *J. Electroanal. Chem.* **196** (1985) 339.
[14] J. Zagal, P. Bindra and E. Yeager, *J. Electrochem. Soc.* **127** (1980) 1506.
[15] D. A. Gough and J. K. Leypoldt, *Anal. Chem.* **51** (1979) 439.
[16] C. P. Andrieur and J. M. Saveant, *J. Electroanal. Chem.* **134** (1982) 163.
[17] D. R. Lawson, L. D. Whiteley and C. R. Martin, *J. Electrochem. Soc.* **135** (1988) 2247.
[18] L. Morcos and E. Yeager, *Electrochim. Acta* **15** (1970) 953.
[19] H. Jahnke, M., Schonborn and G. Zimmermann, *Topics in Current Chemistry* **135** (1976) 61.
[20] Y. Kurimura, E. Tauchida and M. Kaneko, *J. Polym. Sci.* **9** (1971) 3511.
[21] A. Bard and L. R. Faulkner; in 'Electrochemical Methods, Fundamentals and Applications', Ch. 6, p. 213, John Wiley & Sons, New York (1980).